Pharmacogn. Mag.
A multifaceted peer reviewed journal in the field of Pharmacognosy and Natural Products
www.phcog.com | www.phcog.net

ORIGINAL ARTICLE

Tetrahydronaphthalene Lignan Glucoside from *Crataeva nurvala*: Apoptotic Induction, Antimigration, and *in silico* Analysis

Nandan Sarkar, Puneet Kacker[1], Hina Amin[2], Priyanka Narad, Anindya Goswami[2], Sabari Ghosal

Centre for Plant and Environmental Biotechnology, Amity Institute of Biotechnology, Amity University, Noida, Uttar Pradesh, [1]Excelra Knowledge Solutions Private Limited, Hyderabad, Telangana, [2]Indian Institute of Integrative Medicine, Jammu, Jammu and Kashmir, India

Submitted: 10-12-2018 Revised: 22-01-2019 Published: 26-08-2019

ABSTRACT

Background: *Crataeva nurvala* is an important plant having wide application in Ayurveda and Siddha. It is extensively used in formulations for patients suffering from benign prostatic hyperplasia. **Objective:** Isolation, characterization, and evaluation of cytotoxic activity of bioactive fraction of *C. nurvala* and identification of molecular target prediction by suitable method. **Materials and Methods:** Gravity column chromatography followed by HPLC of the bioactive *n*-butanol fraction afforded compound 1. Besides cell proliferation, apoptotic index and cell migration were studied to determine the efficacy of the compound against cancer cells. **Results:** The cell cycle analysis revealed that the compound 1 showing apoptosis inducing property through G2/M arrest and mitotic inhibition. Besides, clonogenic assay and wound healing assay demonstrated that the compound could decrease the ability of colony formation and cell migration in a significant way. However, limited availability of the compound impelled us to undertake *in silico* studies to predictprobable protein targets. This resulted in the identification of IGF1R with highest docking score of −10.0 in preference to four other protein targets (EGFR, AKT1, AKT2, and BCL2) of receptor tyrosine kinase domain (RTKs). As insulin receptor R (Insulin receptor) of tyrosine kinase domain maintains high resemblance with IGF1R, molecular docking was also conducted on the same target. The insignificant docking score suggested specificity of the compound toward IGF1R. **Conclusion:** The study concluded that; (+)-lyoniresino 1-2a-0-β-D-glucopyranoside is a promising apoptosis inducing agent. Molecular modeling of the compound against five crucial protein targets of RTKs suggested that IGF1R could be the probable protein target for the compound.

Key words: (+)-lyoniresinol-2a-O-β-D-glucopyranoside, apoptosis, *Crataeva nurvala*, IGF1R, tetrahydronaphthalene-lignan

SUMMARY

- Bioassay-guided fractionation of *Crataeva nurvala* leads to the isolation of (+)-lyoniresinol-2a-O-β-D-glucopyranoside with significant apoptosis inducing property
- To see the efficacy of the compound in growth kinetics, colony formation assay wound healing assay, and clonogenic assay were performed
- Molecular docking study was conducted to predict the probable protein target.

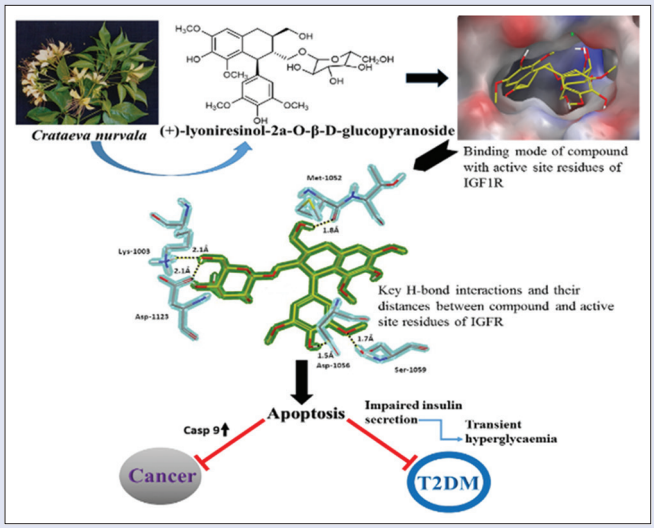

Abbreviations used: BPH: Benign prostatic hyperplasia; Et_2O: Diethyl ether; *n*-BuOH: *n*-butanol; ECACC: European Collection of Authenticated Cell Cultures; FBS: Fetal bovine serum; MEM: Minimum essential medium; HUVECs: Primary human umbilical vein endothelial cells; MTT: 5-Dipheny1tetrazolium bromide; DMSO: Dimethyl sulfoxide; OD: Optical density; PDB: Protein data bank; RTKs: Receptors of tyrosine kinase domain; BMI: Benzimidazole inhibitor; InsR: Insulin receptor; TKIs: Tyrosine kinase inhibitors.

Correspondence:

Prof. Sabari Ghosal,
Centre for Plant and Environmental Biotechnology, Amity Institute of Biotechnology, Amity University, Sector 125, Noida - 201 303, Uttar Pradesh, India.
E-mail: sabarighosal@gmail.com
DOI: 10.4103/pm.pm_624_18

Access this article online
Website: www.phcog.com
Quick Response Code:

INTRODUCTION

Crataeva nurvala Buch. is one of the eleven species of *Capparaceae* family. In traditional medicine, it is used as anticancer, antifertility, anti-arthritic, antitumor, hepatoprotective, anti-inflammatory, and cardioprotective agent.[1] "Himplasia" a polyherbal composition introduced by Himalaya Herbal Health Care Company in 2002, for patients suffering from benign prostatic hyperplasia (BPH) contained *C. nurvala*, as a major constituent.[2] The *n*-hexane and ethanolic extract of the plant is reported to have significant hyperglycemic activity in alloxan-induced rat

This is an open access journal, and articles are distributed under the terms of the Creative Commons Attribution-NonCommercial-ShareAlike 4.0 License, which allows others to remix, tweak, and build upon the work non-commercially, as long as appropriate credit is given and the new creations are licensed under the identical terms.

For reprints contact: reprints@medknow.com

Cite this article as: Sarkar N, Kacker P, Amin H, Narad P, Goswami A, Ghosal S. Tetrahydronaphthalene lignan glucoside from *Crataeva nurvala*: Apoptotic induction, antimigration, and *in silico* analysis. Phcog Mag 2019;15:S307-12.

model,[3] also the ethanolic extract of the plant showed IC_{50} in the range of (10–20 µg/ml) against human cervical cancer (HeLa), Human Lung carcinoma (A549) and MDA-MB (Human adenocarcinoma, mammary gland) cells.[4] The phytochemical studies revealed that the plant contains stigmasterol, cabadicine, β-sitosterol, betulinic acid, and lupeol as major chemical constituents.[5,6]

As a part of our project, the stem bark of the plant was investigated for cytotoxic activity by bioassay-guided fractionation. The methanolic extract was fractionated into diethyl ether (Et_2O) and *n*-butanol (*n*-BuOH) fraction and was evaluated against HeLa, human breast cancer (MCF-7), and human prostate cancer (PC-3) cells. All the Fractions were effective against PC-3 and HeLa cells while were ineffective against MCF-7 cells. In our previous study, we reported two cytotoxic compounds, namely crataemine and crataenoside from Et_2O and *n*-BuOH fractions, respectively [Figure 1]. In the present study, we isolated another compound from the *n*-BuOH fraction with the most significant cytotoxic activity. The structure of the compound was elucidated by HR-ESI-MS and NMR data analysis.

Wound healing assay and colony formation assay were performed to determine the effect of the compound on the growth kinetics of cancer cells. The apoptosis-inducing property was determined by cell cycle analysis and 4, 6-Diamidino-2-phenylindole (DAPI) staining against, HeLa and PC-3 cells. As the compound was obtained in limited quantity, *in silico* approach was adapted to predict the target. It is well established that kinases are involved in numerous cell-signaling cascades and have been implicated in oncogenesis and tumor progression through their aberrant regulation or overexpression. Hence, to predict probable drug target for the compound molecular docking was conducted against five key receptors of tyrosine kinase domain (RTK).

MATERIALS AND METHODS

General

Bruker spectrometer (125/600 MHz) NMR was used using TMS as internal standard. Agilent-6220 accurate mass LC-TOF system attached with Agilent 1200 Series was used for HR-ESI-MS. HPLC was conducted on the Shimadzu semi-prep LC controller system. RP-18 prep-ODS column (10 µm, 10 mm × 250 mm) with PDA detector (SPD-M20A). Silica gel (60, 120–200, and 240–360 mesh) was used for silica column chromatography. Pre-coated silica gel 60 GF_{254} plates and HPTLC (Merck) plates were used for analysis. The spots were observed under ultraviolet (UV) light (254 and 360 nm), and anisaldehyde-sulfuric acid was used as spraying reagent.

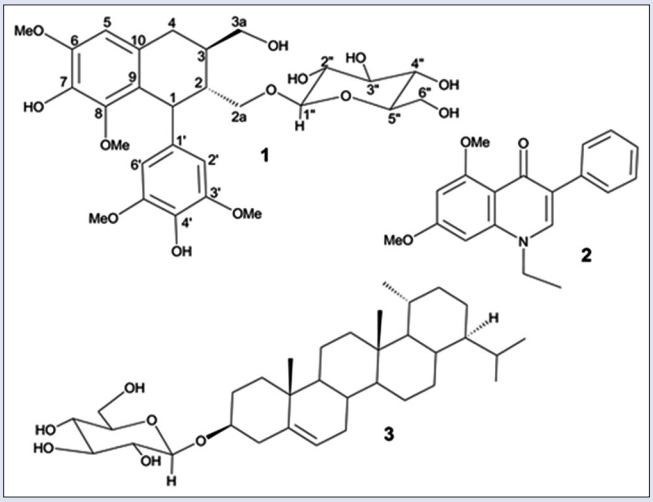

Figure 1: Chemical structures of (+)-lyoniresinol-2a-O-β-D-glucopyranoside (1), crataemine (2) and crataenoside (3)

Plant material

The plant part was procured from a registered vendor namely "Accolent Dried Herbs" Parkvale Street, Victoria Point, Queensland 4165, Australia, and authentication was performed by Dr. M. P. Sharma, Professor, Department of Botany, Hamdard University, New Delhi. A voucher specimen (SG/01/2010) has been preserved in the herbarium of Amity University, Noida, India.

Extraction, isolation, and characterization

The dried stem bark of the plant (0.30 kg) was extracted with MeOH: H_2O (9:1; 1 L × 3 h × 24 h) followed by H_2O (0.5 L) at room temperature. The concentrated MeOH extract was fractionated into Et_2O (1.5 L, 7.9 g) and *n*-BuOH (1 L, 1.9 g). Chromatography of Et_2O fraction afforded lupeol, stigmasterol, and crataemine.[2] Further, flash chromatography of *n*-BuOH soluble fraction with DCM and 5% stepwise gradient of MeOH, afforded six fractions (80 mL; S-1–S-6). Fraction S-2 afforded crataenoside.[3]

In the second phase, the chromatographic separation was conducted with subfraction S-5, as it exhibited interesting TLC profile and most significant biological activity. Flash column chromatography of S-5 with 20% MeOH-DCM afforded compound 1 [Figure 1] in semi-purified form, which was purified further on preparative column (C-18, 10 mm × 250 mm) using CH_3CN-H_2O (70:30; 25 min, 5 ml/min) as eluent solvents. The compound 1 was obtained (15 mg, 0.006%) as a white amorphous solidat 15.4 min (t_R) run time.

Acid hydrolysis of compound 1

The hydrolysis of 1 was performed by the method described previously.[7] Briefly, 5 mg of sample was heated at 60°C for 60 min after dissolving in 95% ethanol in 2 N HCl, and the residue was extracted thrice with EtOAc. The pooled EtOAc fractions provided the aglycone and the aqueous layer after neutralization with Amberlite MB-3 (Organo Co.) produced the monosaccharide residue. The rest residue was analyzed by HPTLC developed with 2 mMNaOAc (17:3, v/v) and Me_2CO and the spots were detected by spraying with 0.2% naphthoresorcinol in Me_2CO and 3 N H_3PO_4 followed by heating at 105°C for 3 min (R_f 0.7). D-Glucose was used as standard.

(+)-Lyoniresino1-2α-O-β-d-glucopyranoside (1)

Amorphous white powder; UV (MeOH), λ_{max}, nm (log ε): 276 (3.68).

^{1}H NMR (600 MHz, CD_3OD): δ 6.46 (s, 1H, H-5), 6.31 (s, 2H, H-2′, H-6′), 4.29 (d, 1H, *J* = 5.9 Hz, H-1), 4.17 (d, 1H, *J* = 7.8 Hz, H-1′′), 3.85(m, H-2a), 3.73 (s, 3H, 6-OMe), 3.67 (s, 6H, 3′,5′-OMe), 3.54 (m, H-3a), 3.54 (dd, 1, *J* = 10.9, 6.6 Hz, Hb-3a), 3.54–3.27 (complex m, H-2′′, 3′′, 4′′, 5′′, 6′′), 3.27(s, 3H, 8-OMe), 2.61(dd, 1, *J* = 15.2, 4.7 Hz, Hb-4), 2.52 (dd, 1, *J* = 15.2, 11.8 Hz, Ha-4), 2.01 (m, 1H, H-2), 1.64 (m, 1H, H-3).

^{13}C NMR (125 MHz, CD_3OD): δ 146.9 (C-3′, 5′), 146.6 (C-6), 145.6 (C-8), 137.2 (C-1′), 136.9 (C-7), 132.5 (C-4′), 128.3 (C-10), 124.5 (C-9),106.0(C-5), 105.0 (C-2′, 6′), 102.8 (C-1′′), 76.2 (C-3′′), 75.9 (C-5′′),73.2 (C-2′′), 69.7 (C-4′′), 70.0 (C-2a), 64.6 (C-3a), 61.0 (C-6′′), 58.7 (8-OMe), 56.8 (3′,5′-OMe), 56.6 (6-OMe), 44.9 (C-2),40.9 (C-1), 38.8 (C-3), 32.0 (C-4); HR-ESI-MS (+ve): m/z calc. for $C_{28}H_{38}O_{13}$ 605.2301 (M + Na) and 1187.4602 [2M + Na]; found, 605.2273 (M + Na) + and1187.4557 [2M + Na] +, respectively.

Biological activity

Cell culture

The cells were procured from the European Collection of Cell Culture. Minimum Essential Medium, fetal bovine serum, RPMI-1640, streptomycin, penicillin G, and trypsin-EDTA were obtained from Invitrogen Corp. Primary Human Umbilical Vein Endothelial Cells were cultured in endothelial growth medium obtained from invitrogen. 5-Diphenyltetrazolium bromide (MTT), staurosporine, paraformaldehyde, camptothecin, etoposide, podophyllotoxin, dimethyl sulfoxide (DMSO), UltraCruz DAPI mounting medium, and Propidium iodide were purchased from Santa Cruz Biotechnology Inc. (Santa Cruz, CA, USA).

Cell proliferation assay

Cell viability was conducted by MTT assay.[8] In brief, the cancer cells (3×10^3 cells/well) were plated in 96 well plates with different concentrations of 1 in triplicate. After incubation of 48 h, MTT solution was added and was further incubated for 4 at 37°C. The intensity of color developed was calculated by optical density.

Apoptosis by DAPI staining

Adherent PC-3 cells (1×10^5 cells/well), treated with 1 were harvested by trypsin digestion and washed twice with chilled phosphate buffered saline (PBS). Further Cells were fixed with paraformaldehyde (4%) followed by incubation with DAPI containing medium for 15 min at room temperature. Apoptosis was noticed by fluorescence microscopy (×100).[9]

Cell cycle analysis

PC-3 cells were plated in 6 well plates (5×10^5 cells/well) by treating with different concentrations of 1 for 24 h. After that, the cells were collected by trypsinization and washed with PBS. Thereafter, cells were incubated in hypotonic solution (25 mg/ml propidium iodide, 0.1% sodium citrate, 40 mg RNase-A, and 0.03% Triton-X100,) at room temperature for 25 min and then assimilated for FACS analysis.[10]

Wound healing assay

Briefly, PC-3 and MCF-7(data not shown) cells were seeded in 6 well plates (5.5×10^5 cells/well) and left for grown over night to form a confluent monolayer. Thereafter, an artificial wound was made using a sterile pipette tip (200 ml) after 24 h of serum starvation and washed with serum-free medium to remove detached and floated cells. A photograph was noted (time 0 h). Thereafter, the cells were consecutively treated in a medium containing low serum (1%), in the presence of various concentrations of 1 for 24 h. The wounded areas were gradually again photographed with Olympus c-7070 with 700M camera (100X magnification). The percentage of wound closure was assessed by the following equation: wound closure % = (1 – [wound area at t_1/wound area at t_0] × 100%), where t_1 is the time after wounding and t_0 is the time immediately after wounding.[11]

Clonogenic assay

Briefly, the cultured plates of PC-3 cells (1×10^3 cells/well) were treated with different concentration of the compound 1 along with vehicle DMSO for 5 days in CO_2 incubator (5%) at 37°C. The colonies formed were fixed with paraformaldehyde (4%) and stained with crystal violet solution (0.5%).[12] Stained colonies were erratically counted from the observed fields ($n = 3$). A photographed was taken with Olympus c-7070 wide 700M inverted microscope camera.

Cell cytotoxicity assay

The cell cytotoxicity was performed by MTT assay against BPH-1 cells. An untreated group was used as a negative control. The concentration of the compound required to cause a half-maximal inhibition of cell proliferation (IC_{50}) was determined.

Molecular modeling

The potential list of five targets [Table 1] was generated from experimentally known crystal structures of the targets. Alternative binding sites known on the same target were also considered in the simulation study, to cover all possible binding modalities of the ligand. Molecular modeling calculations were performed by considering all possible bindings modalities of the ligand and six ligand binding sites were explored by molecular modeling procedures.

Ligand preparation

The two dimensional (2D) structure of 1 was made using the SMILES provided on the Chemical Entities of Biological Interest database (CHEBI ID: 66606) website using sketcher functionality of Schrodinger Maestro. Ligand preparation was carried out using the LigPrep application of Schrodinger's Maestro Suite. Software's default options were used to prepare the ligand's 3D structure. The same structure was kept for all docking calculations.

Target structures preparation

Experimental coordinate files of all five protein targets, including six protein data bank (PDB) structures to address six ligand binding sites, were taken from PDB (RCSB PDB). The total number of six targets was explored through extra-precision molecular docking simulation. After protein preparation, grid maps were generated using Glide application of maestro. Grids were generated using the reference of known co-crystallized compound present in each target structure. The assessment of the probable binding affinity and calculation of ligand binding mode for each of its potential target is made using highly accurate XP Glide docking score (G-score). G-score is an experimental scoring function used to estimate the binding free energy of a ligand. It denotes, mainly force field (electrostatic, van der Waals) contributions and terms, rewarding or penalizing interactions, which influence ligand binding. The negative value of G-score is directly proportional to the potency of the compound. The docking poses, including the ligand contact maps, were analyzed using the same condition. Docking was carried out using XP mode, and pose-viewer file was saved in each docking run for further analysis.

RESULTS AND DISCUSSION

Characterization of the compound

The HR-ESI-MS of compound 1 exhibited (M + Na) + ion peak at m/z 605.2273 indicating the molecular formula to be $C_{28}H_{38}O_{13}$ (calc.

Table 1: Docking scores of compounds 1 against six ligand binding sites of five protein targets of receptor tyrosine kinases domain

Target name	PDB ID	XP dock score
IGFR-main site	2OJ9	−10.0
IGFR-allosteric site	3LW0	−8.2
AKT2	3D0E	−7.5
EGFR	3POZ	−6.6
Bcl-2	4LXD	−6.5
AKT1	4GV1	−6.0
InsR	3EKN	−5.7

PDB: Protein data bank

605.2301). The ^{1}H NMR spectra showed characteristics aromatic protons appearing at δ 6.31 (2H, s) corresponding to a tetra-substituted 1,3,4,5-phenyl moiety; an aromatic singlet at δ 6.46 representing a penta-substituted benzenoid residue; one anomeric proton at δ 4.17 (1H, d, J = 7. 8 Hz); an aliphatic proton at δ 4.29 (1H, d, J = 5.9 Hz); and four methoxy protons at δ 3.67 (6H, s), δ 3.73 (3H, s) and 3.54 (3H, s). The ^{13}C NMR signals at δ 102.8, 76.2, 75.9, 73.2, 69.7, and 61.0 along with large coupling constant of the anomeric proton (7.8 Hz) expressing the presence of a β-D-glucopyranoside ring linked to an aglycone moiety. In addition, two identical methine carbons at δ 105.0 (C-2′ and C-6′) and three quaternary carbons at δ 146.9 (C-3′ and C-5′) and δ 132.5 (C-4′) along with two identical methoxyl carbons at δ 56.9 suggested the presence of 3,5 dimethoxy-4-hydroxy substituted phenyl moiety in the compound. ^{13}C NMR spectrum of compound 1 also displayed the characteristic peak of a penta-substituted phenyl moiety where, two consecutive positions were attached with aliphatic carbons (δ 124.5 and 128.3) and rest three adjacent positions (δ 136.9, 145.6, and 146.6) were occupied by three oxygenated functionalities. In addition, three methine carbons (δ 38.8, 40.9 and 44.9), two oxymethylene (δ 64.6, 70.2) and one methylene (δ 32.0) carbon in DEPT spectra suggested the presence of aryl tetralin lignin. The β-D-glucopyranoside unit attached to a methylene hydroxyl group was suggested by the appearance of an anomeric proton and carbon at δ4.2 and δ 70.2 along with oxymethylene carbon at δ 70.0. The final structure of the compound was established by ^{1}H-^{1}H COSY, NOESY, HMQC, and HMBC spectral analysis. Moreover, the presence of glucose was confirmed by acid hydrolysis of 1, with 2 N HCl and was confirmed by co-HPTLC with the authentic sample. All these spectral and analytical data were compared with reported literature and the structure of compound 1was confirmed as (+)-lyor esinol-2a-O-β-D-glucopyranoside, a tetrahydronaphthalene lignin glucoside. This is the first report of the occurrence of the compound in *C. nurvala*.

Biological activity

Compound 1 exhibited promising antiproliferative activity against PC-3 and Hela cells with IC_{50} values of 7 and 8 μM, respectively [Figure 2], where the compound was neutral against MCF-7 cells; hence, further analysis was conducted with those cells only.

Cell cycle analysis revealed that 1 induced apoptosis in PC-3 cells within 24 h of incubation, comparable to positive control staurosporine, as represented in Figure 3a and b. The occurrence of apoptosis has been presented with red arrows indicating chromatin condensation. Thereafter, flow cytometric analysis was conducted to measure apoptotic index and cellular DNA content in various phases of the cell as shown in Figure 3c and d. Interestingly, 1 observed 28.7%, 54.7%, and 78.9% apoptotic cells at 1 μM, 5 μM and 10 μM concentrations compared to 70.8% for 1 μM concentration of positive control camptothecin. The flow cytometric data expressed a steady-state G2/M arrest in cells with 10 μM concentration of 1 (78.9%) compared to 1 μM (70.8%) of positive control camptothecin. Together, these results showed that 1 could act as apoptosis inducer through G2/M arrest and mitotic inhibition.

Compound	PC-3 IC_{50} (μM)	HeLa IC_{50} (μM)	BPH-1 IC_{50} (μM)
Compound 1	7	8	78.023
Podophyllotoxin	0.034	0.10	67.43
Etoposide	2.94	0.23	71.51

a

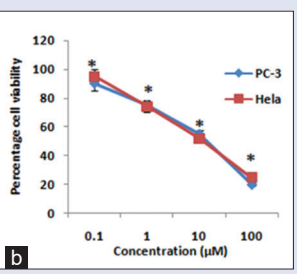

b

Figure 2: (a) Cell viability of1expressed in IC_{50} values against prostate cancer 3, human cervical cancer, and Benign prostatic hyperplasia-1 cells. Positive controls were podophyllotoxin and etoposide. (b) Plot of cell viability versus concentration to determine the antiproliferative activity of 1

Wound healing assay revealed that the vehicle DMSO-treated cells (control) could completely fill in the cleared area and 1, 5, and 10 μM treated compound 1 significantly ($P < 0.05$) inhibited the migration of PC-3 cells [Figure 3e]. Compounds efficacy on the growth kinetics of cells was inspected by colony formation assay [Figure 3f]. Sublethal dose of 1 was able to decrease the colony formation ability of the cells in a statistically significant manner ($P < 0.05$). All these experiments clearly revealed that the compound induces apoptosis and cell migration significantly.

To determine cell cytotoxicity of the compound, different concentrations of the compound was treated against BPH-1 cells. The cell cytotoxicity results clearly demonstrated that the compound has the least cytotoxic activity on the non-malignant cells.

Molecular modeling

Selectivity and specificity of an active compound is crucial for drug development. Hence, due to the absence of a sufficient amount of compound, molecular modeling approach was adapted to identify the probable protein targets. Many of the signals of oncogenesis are regulated by RTKs. These RTKs are membrane-spanning proteins with intrinsic phosphotyrosine kinase activity.[13] Their activity is normally tightly regulated. In the absence of ligand, TRKs reside in the plasma membrane as inactive enzymes. Binding of ligand promotes receptor dimerization and a change in conformation that leads to activation of the kinase and transphosphorylation of the receptor on specific tyrosine residues. In addition to alterations in the RTK, aberrant degradation of RTKs is related with various cancers, accentuating the importance of this mechanism of RTK regulation. Hence, we conducted molecular docking of compound 1 against five crucial protein targets of RTKs namely IGF1R (catalytic and allosteric binding site), EGFR, AKT1 and AKT2 and BCL 2 comprising six ligand binding sites to explore the binding mode of the compound. The overall docking score on these targets lied between 6 and 10, suggesting that the binding affinity varied significantly among the listed targets [Table 1] and the most significant docking score of −10.0 and −8.2 was observed against the catalytic and allosteric binding site of IGF1R.

The catalytic site of IGF1R (PDB ID: 2OJ9) was established from the protein complex co-crystallized with benzimidazole inhibitor (BMI). The potent inhibitor BMI (IC_{50}390 nM) was used as a positive control in this simulation.[14] On the basis of docking score and binding mode analysis against six protein targets, the catalytic (−10.0) and allosteric binding (−8.2) sites of IGF1R was considered as the most probable binging site [Figure 4a]. The best docking pose [Figure 4d] of 1 indicated that the binding mode was similar to BMI [Figure 4b and c] with five strong H-bond interactions ranging from 1.5 Å to 2.1 Å. Considerably higher number of H-bonds were observed (13 oxygen) at the catalytic pocket however, the most important H-bond between BMI and Met-1052 residue was maintained by 1. Four strong interactions with Lys-1003, Asp-1123, Asp-1056, and Ser-1059 residues of the catalytic site with 1 further strengthen the prediction. Although a specific H-bond between Glu-1050 residue and compound 1 was missing, the total number of H-bonds and optimal size played an important role in the stability of the complex. The best docking pose of 1 at the allosteric pocket (3 LWO) showed that the crucial H-bond between Val1063 and the ligand was

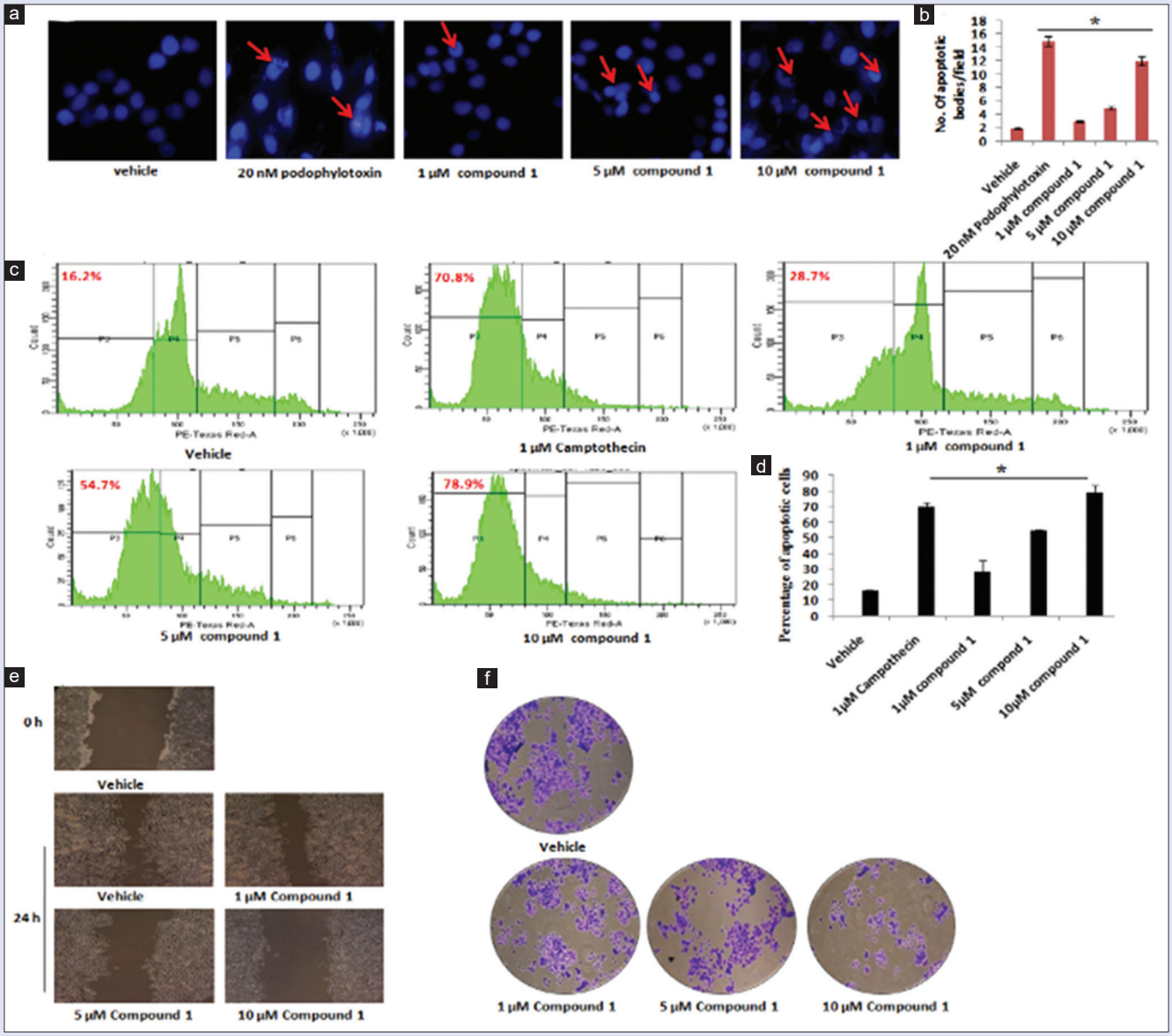

Figure 3: The assessment of cell death and motility of 1, vehicle dimethyl sulfoxide and positive control staurosporine (25 nM) or camptothecin (1 mM), (a and b) prostate cancer 3 cells (5×10^4) after treatment, were fixed, stained with nuclear DAPI reagent. Apoptotic nuclei were characterized and photographed under a fluorescence microscope (×100), and data were generated from three independent experiments. (c and d) Cell cycle analysis to determine cell cycle phase distribution, (e) wound healing assay (0.5×10^5 cells/well) to assess the degree of wound healing after compound 1 treatment, (f) Colony formation assay against prostate cancer 3 cells (1×10^3 cells/well), in presence of compound 1. After 7 days, the cells were stained with crystal violet. The number of stained cells per colony was counted randomly, and images were captured in ×100 under an inverted microscope. Data were calculated from three independent experiments *$P < 0.05$

missing [Figure 4e], which could alter the shape of the allosteric pocket and makes it less viable for effective binding.

Nearly 84% sequence similarity of insulin receptor (InsR), another important RTK prompted us to extend molecular docking exercise against InsR (PDB ID: 3EKN) as well. The crystal structure of InsR was extracted from pyrrolopyrimidin complex where pyrrolo-pyrimidin acts as a highly potent (IC_{50} = 2nM) inhibitor.[15] The lowest docking score of −5.7 strengthened our hypothesis that 1 works specifically for IGF1R and not InsR.

Several approaches have been conducted to study signaling at IGF1R, which shows variant in different mechanisms of action, target inhibition, and pharmacological aspects. One of these approaches involves IGF1R tyrosine kinase inhibitors. Few molecules, following this route are under clinical trials.[16] Hence, the isolation of compound 1 from abundantly available natural resources and subsequent evaluation of activity against the catalytic site of IGF1R could provide very important information at the cellular level.

CONCLUSION

The present study identified (+)-lyoniresino1-2a-O-β-D-glucopyra noside (1), isolated from the stem bark of *C. nurvala* with significant antiproliferative, apoptotic, and cell migratory activity against PC-3 and HeLa cells. Molecular docking study conducted against five protein targets of RTKs identified IGF1R as a potential target. This observation could further be verified by *in vitro* experiments to establish its potential as a drug candidate.

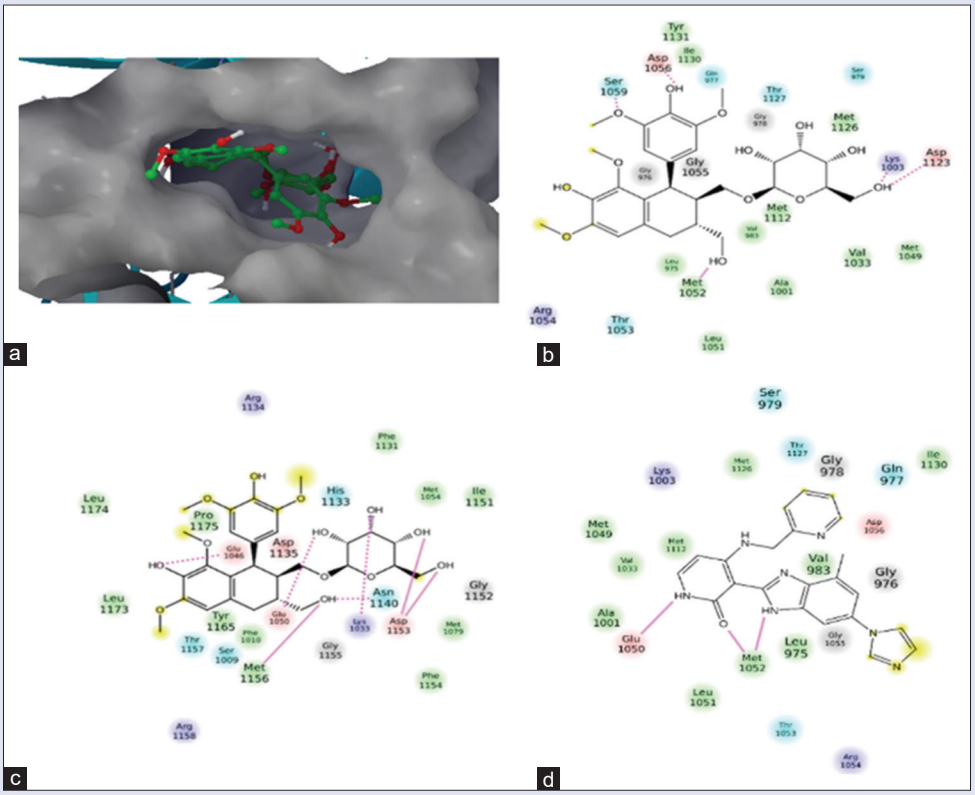

Figure 4: Docking results (a) Surface representation (side-view) of 1 at the main binding site of IGF1R (Protein data bank ID 2OJ9) (b) Key interactions of1 and IGF1R at main site, (c) Key interactions of 1 at the allosteric site (Protein data bank ID 3 LW0). Interaction map shows the absence of key residue (Val1063) even in the close vicinity of 1. (d) Key interactions between benzimidazole inhibitor and active site residues of IGF1R (Protein data bank ID 2OJ9). Legend: solid pink lines-interactions with amino acid backbone, broken pink lines-interactions with amino acid side-chains, residues color based on their nature

Financial support and sponsorship

Authors are thankful to the Department of Science and Technology, Government of India for financial assistance, Dr. Ajay Kumar, AIRF-JNU, Delhi, for helping in NMR and Dr. A. K. Chauhan, President of Amity University for his constant impetus and inspiration.

Conflicts of interest

There are no conflicts of interest.

REFERENCES

1. Sinha S, Mishra P, Amin H, Rah B, Nayak D, Goswami A, *et al.* A new cytotoxic quinolone alkaloid and a pentacyclic steroidal glycoside from the stem bark of *Crataeva nurvala*: Study of anti-proliferative and apoptosis inducing property. Eur J Med Chem 2013;60:490-6.
2. Shrivastava A, Gupta VB. Various treatment options for benign prostatic hyperplasia: A current update. J Midlife Health 2012;3:10-9.
3. Sikarwar MS, Patil MB. Antidiabetic activity of *Crataeva nurvala* stem bark extracts in alloxan-induced diabetic rats. J Pharm Bioallied Sci 2010;2:18-21.
4. Wagh NS, Gaikwad NJ. Evaluation of anti-cancer activity of bark of *Crataeva nurvala* buch. IJPSR 2014;11:4851-7.
5. Ahmad VU, Fizza K, Amber AU, Arif S. Cadabicine and cadabicine diacetate from *Crataeva nurvala* and *Cadaba farinose*. J Nat Prod 1987;50:1186-3.
6. Parvin S, Kader MA, Muhit MA, Haque ME, Mosaddik MA, Wahed MI, *et al.* Triterpenoids and phytosteroids from stem bark of *Crataeva nurvala* buch ham. JAPS 2011;9:47-4.
7. Tung YT, Cheng KC, Ho ST, Chen YL, Wu TL, Hung KC, *et al.* Comparison and characterization of the antioxidant potential of 3 wild grapes – *Vitis thunbergii, V. flexuosa*, and *V. kelungeusis*. J Food Sci 2011;76:C701-6.
8. Koppikar SJ, Choudhari AS, Suryavanshi SA, Kumari S, Chattopadhyay S, Kaul-Ghanekar R, *et al.* Aqueous cinnamon extract (ACE-c) from the bark of *Cinnamomum cassia* causes apoptosis in human cervical cancer cell line (SiHa) through loss of mitochondrial membrane potential. BMC Cancer 2010;10:210.
9. Wu PP, Chung HW, Liu KC, Wu RS, Yang JS, Tang NY, *et al.* Diallyl sulfide induces cell cycle arrest and apoptosis in HeLa human cervical cancer cells through the p53, caspase- and mitochondria-dependent pathways. Int J Oncol 2011;38:1605-13.
10. Zhu W, Depamphilis ML. Selective killing of cancer cells by suppression of geminin activity. Cancer Res 2009;69:4870-7.
11. Liang XJ, Choi Y, Sackett DL, Park JK. Nitrosoureas inhibit the stathmin-mediated migration and invasion of malignant glioma cells. Cancer Res 2008;68:5267-72.
12. Kaul R, Mukherjee S, Ahmed F, Bhat MK, Chhipa R, Galande S, *et al.* Direct interaction with and activation of p53 by SMAR1 retards cell-cycle progression at G2/M phase and delays tumor growth in mice. Int J Cancer 2003;103:606-15.
13. Sangwan V, Park M. Receptor tyrosine kinases: Role in cancer progression. Curr Oncol 2006;13:191-3.
14. Wang SY, Kuo YH, Chang HN, Kang PL, Tsay HS, Lin KF, *et al.* Profiling and characterization antioxidant activities in *Anoectochilus* formosanus hayata. J Agric Food Chem 2002;50:1859-65.
15. Fan C, Huang YX, Bao YL, Sun LG, Wu Y, Yu CL, *et al.* Virtual screening of specific insulin-like growth factor 1 receptor (IGF1R) inhibitors from the national cancer institute (NCI) molecular database. Int J Mol Sci 2012;13:17185-209.
16. Chen HX, Sharon E. IGF-1R as an anti-cancer target – Trials and tribulations. Chin J Cancer 2013;32:242-52.